Journal of Applied Fluid Mechanics, Vol. 11, No. 1, pp. 217-224, 2018.
Available online at www.jafmonline.net, ISSN 1735-3572, EISSN 1735-3645.
DOI: 10.29252/jafm.11.01.27494

Steady-State Experiment and Simulation of Intake Ports in a Four-Valve Direct Injection Diesel Engine

D. W. Jia, X. W. Deng and J. L. Lei †

Yunnan Key Laboratory of Internal Combustion Engine, Kunming University of Science and Technology, Kunming 650500, China

†*Corresponding Author Email: 22972489@qq.com*

(Received December 14, 2016; accepted September 3, 2017)

ABSTRACT

In order to analyze intake port flow characteristics of a four-valve direct injection (DI) diesel engine, steady-state flow bench experiments and numerical simulations method were coupled to investigate the following four combined intake ports: (1) helical port (left) and tangential port (right); (2) tangential port (left) and helical port (right); (3) helical port (left) port and helical (right); and (4) tangential port (left) and tangential (right) port. Results show that the simulation of port flow coefficients matches experimental findings very well, and the port coefficients of the above four combinations do not vary much, but their swirl ratios are very different. Specifically, when the valve lift is the maximum, the swirl ratio of the combination of "helical and tangential" is the greatest among the four combinations, and the swirl ratio of "tangential and tangential" is the minimum. And the3D fluid simulation method and steady-state experiment are important means to investigate the flow characteristics of the combined intake ports.

Keywords: Four-valve DI diesel engine; Flow characteristics; Combined intake ports; Steady-state experiment; Simulation.

NOMENCLATURE

A_V	inner cross-section area of the valve seat	$(SR)_m$	average swirl ratio
$c(\alpha)$	instantaneous velocity of the piston		
$c(\alpha)$	average velocity of the piston	ρ_0	ambient air density
d_V	inner diameter of the valve seat	ρ_m	average density of gas
$\dot{m}_{theo}$	theoretical gas mass flow rate	μ_m	average flow coefficient
$\dot{m}_{actual}$	actual gas mass flow rate	ρ	gas density in the cylinder
n_E	simulated speed of the diesel engine	Δp	pressure differential across the valve or between the inlet and outlet of the port
n_D	the speed of the vane anemometer	μ	the ratio of actual air mass flow rate to theoretical air mass flow rate
SR	swirl ratio		

1. INTRODUCTION

The performances of an internal combustion engine are usually evaluated on the basis of global parameters such as power, torque, fuel consumption, pollutant and acoustic emissions (Della Torre A *et al*., 2017). At present, the emissions have become the focus of attention, and the intake port is designed to introduce high levels of s "tumble" charge motion (Hartmann F *et al*., 2016), which can improve combustion. And the intake air swirl motion was very important to spark-ignition direct-injection engine (Choi, M *et al*., 2016), but also to the CNG direct injection engine (Zhuang, H *et al*.,2016). So with the diesel engine combustion imposes stringent requirements on in-cylinder mixture formation and flow, well organized air flow in the cylinder is important for enhancing fuel-gas mixing rate and promoting burning rate in the combustion process. With the requirements of improving diesel engine technologies, performance and emissions, the technology of four-valve cylinder head has replaced two-valve head and become a prevailing structure for modern

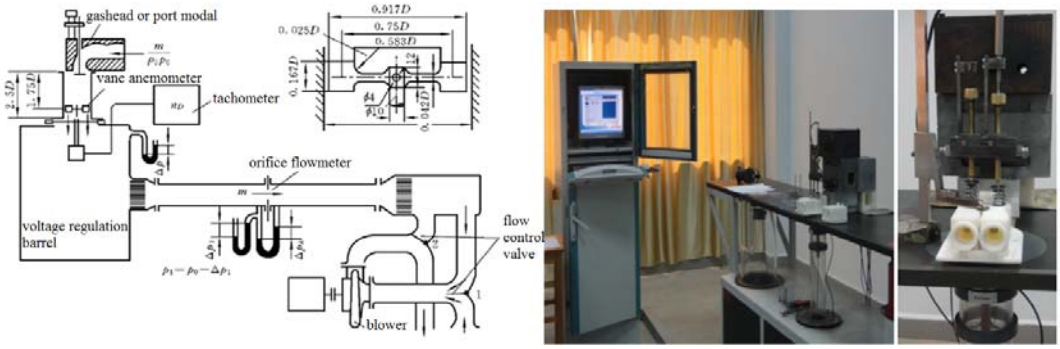

Fig. 1. Steady-state flow bench of intake port testing.

medium-size and small-size high-speed direct injection (DI) diesel engines. Because the air flow patterns of the four-valve head are more complex than those of the two-valve head, the two adjacent intake ports of the four-valve head may interfere each other to affect air flow motion, flow rate, and in-cylinder swirl. Moreover, intake flow characteristics are affected by different shapes of the intake port structure, port position in the cylinder head, and the combination patterns of the two ports. Therefore, in order to develop high efficiency and low emissions four-valve DI diesel engines, it is important to systematically study the effects of different combinations of intake ports on intake flow characteristics (Kawaguchi at al .,2009, Andreatta *et al*.,2008, Li Yufeng at al .,2001, Li Yufeng and Wang Zhong,2004,Lu Z. *et al*.,2014,and Cui L.*et al*.,2015).

In order to resolve the previous research on the flow characteristics of different combined intake ports is not comprehensive, the 3D fluid simulation model and steady-state experiment were coupled in this paper And the 3D models of four different combinations of intake helical port and tangential port were established by using the Unigraphics (UG) software. The AVL CFD software "Fire" was used to simulate their steady-state flow characteristics. Flow coefficients and swirl ratios of these combinations of intake ports at various valve lifts were analyzed and compared with experimental results.

2. STEADY-STATE EXPERIMENT OF INTAKE PORTS

2.1 Testing Equipment

A steady-state flow bench for intake ports was used to simulate the flow processes in the intake ports of an actual diesel engine. As an important approach to investigate diesel intake flow characteristics, such a test can provide evaluation on intake port flow coefficient and swirl ratio for development of diesel engine intake systems and burning mixture formation(Sun Ping *et al* .,2007, Cantore *et al* .,2005, Rathnarajfe *et al*.,2006,Kawashima *et al* .,1998). Steady-state intake flow testing methods include mainly vortex moment of momentum and vane anemometer, and flow rate is usually measured by using standard flow meters.

The steady-state flow bench is shown in Fig. 1, mainly including a pressure regulating box, a valve lift control device, a vane anemometer, and an orifice flow meter. Testing was conducted by using a constant pressure differential method, i.e., keeping a constant pressure differential across the intake valve, and measuring air flow rate and vane anemometer speed (n_D) at different valve lift. The length of the simulated air cylinder was set as 2.5D, where D is cylinder diameter, and vane was positioned at a distance of 1.75D away from the top of the cylinder head. And the parameters of diesel engine were show in Table1.

Table 1 Basic parameters of diesel engine

item(units)		parameters
cylinder number		2
bore ×stroke /mm		80×92
displacement/L		1.85
compression ratio		16.5:1
combustion chamber		ω type
maximum torque /N·m		125
maximum torque speed/r·min-1		2200
rated power /kW		41
rate power speed/ r·min-1		4000
valve timing/crank angle	IVO	14° BTDC
	IVC	52° ABDC
	EVO	32.6°BBDC
	EVC	37.4°ATDC

2.2 Testing Plan

For medium-size and small-size high-speed diesel engines, in order to increase volumetric efficiency and promote sufficient fuel-air mixing, a high swirl ratio is usually required at low-speed low-load conditions. In contrast, at high-speed high-load conditions, a low swirl ratio is required. Therefore, different combinations of intake port structure are potentially needed in order to meet distinct requirements of intake charging at different conditions.

There are many arrangement layouts of intake ports for four-valve-head diesel engines. Different

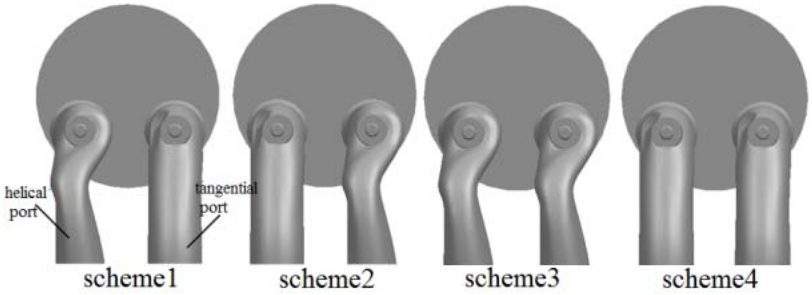

Fig. 2. Different combinations of intake port types.

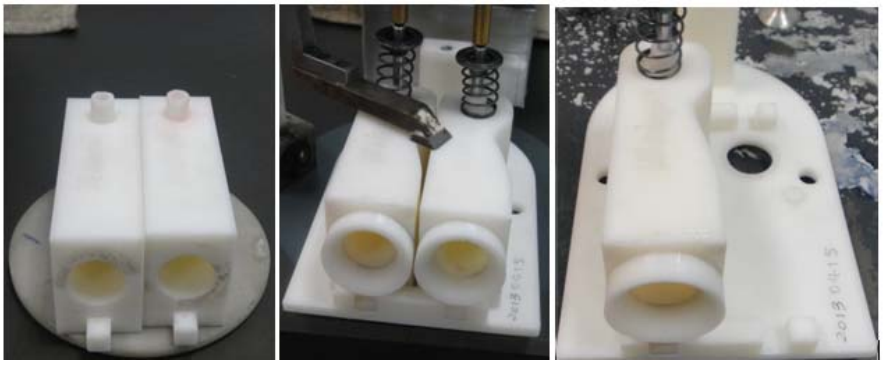

Fig. 3. Prototypes of intake ports.

combinations in type (helical or tangential), angle, or geometry can result in different flow coefficients and swirl ratios. Currently, there are mainly two types of inlet ports, tangential and helical. They have four major combinations as follows (Fig. 2): (1) helical (left) and tangential (right, scheme 1); (2) tangential (left) and helical (right, scheme 2); (3) helical (left) and helical (right, scheme 3); and (4) tangential (left) and tangential (right, scheme 4). The volume of the single tangential port or the helical port was the same in the combined intake ports, which meted the need of the engine of air intake.

The intake port prototypes used in testing were made by rapid prototyping technology. In order to save cost, two helical ports, two tangential ports, and one body deck representing the bottom structure of the cylinder head were separately procured, as show in Fig. 3. A mounting and positioning structure was attached to the body deck, and it allowed combining different ports to form various combinations. Moreover, an inclined flow guiding plane was produced at the entrance of the intake ports in order to better guide the air flow.

The intake ports in this study simulate the ports of a high-speed two-cylinder DI diesel engine, and the basic parameters were shown in Table 1, and the maximum valve lift was 8 mm. The valve lifts used in testing and numerical simulation were set at 1 mm, 2 mm, 3 mm, 4 mm, 5 mm, 6 mm, 7 mm, and 8 mm to investigate port flow characteristics.

2.3 Evaluation Approach

The dimensionless flow coefficient μ and swirl ratio SR defined by AVL were used to evaluate intake port flow capacity at different valve lifts.

The flow coefficient μ is defined as the ratio of actual air mass flow rate to theoretical air mass flow rate:

$$\mu = \frac{\dot{m}_{actual}}{\dot{m}_{theo}} \tag{1}$$

$$\dot{m}_{theo} = A_V \cdot \rho \cdot \sqrt{\frac{2 \cdot \Delta p}{\rho_m}} \tag{2}$$

$$\rho_m = \frac{1}{2}(\rho_0 + \rho) \tag{3}$$

where $A_V = d_V^2 \pi / 4$, $\rho = \rho_0 \cdot [(p_0 - \Delta p)/p_0]^{1/\kappa}$, $\kappa = 1.4$.

The average flow coefficient μ_m is calculated as follows:

$$\mu_m = \frac{1}{\pi} \int_{\alpha=0}^{\alpha=\pi} \mu \sigma d\alpha \tag{4}$$

The swirl ratio SR is calculated as follows:

$$SR = \frac{n_D}{n_E} \tag{5}$$

Intake swirl was measured by using a vane anemometer, as shown in Fig.1. The outer diameter of the vane is equal to 0.917D, and the inner diameter is equal to 0.583D.

The average swirl ratio $(SR)_m$ is calculated as follows:

$$(SR)_m = \left(\frac{n_D}{n_E}\right)_m = \frac{1}{\pi}\int_{\alpha=0}^{\alpha=\pi} \frac{n_D}{n_E}\left(\frac{c(\alpha)}{c_m}\right)^2 d\alpha \quad (6)$$

3. BUILDING SIMULATION MODEL OF INLET PORT FLOW

3.1 Geometry Model and Mesh Generation

In order to analyze intake port flow characteristics, a geometry model was developed. The model consists of a rectangular stabilizing chamber for intake air pressure, two intake ports, two intake valves, two valve seats, and a cylinder, as shown in Fig. 4.

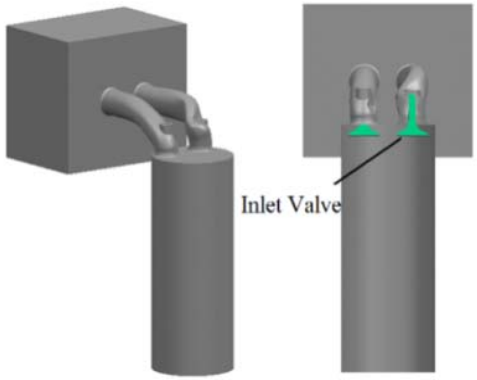

Fig. 4. Intake port geometry model.

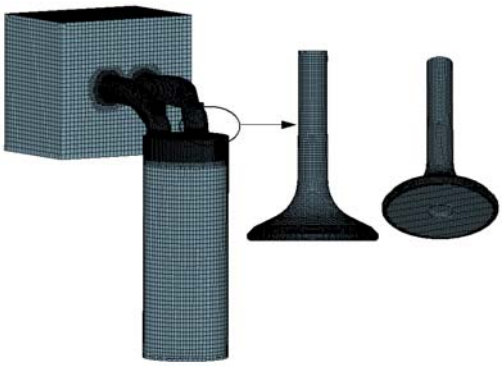

Fig. 5. Mesh generation for intake port model.

Automatic mesh generation was conducted by using the AVL FAME Hybrid pre-treatment function module for the ports. In order to accurately analyze the air flow motion around the valve section, it was necessary to refine the mesh for the valve face and the valve seat, the mesh of the solid model at a valve lift of 8 mm shown in Fig. 5. The mesh consists of Hexahedral, Prism, Pyramid, and Tetrahedron meshes, and the total of the mesh quantity is 570,000, with the hexahedral mesh occupying approximately 90% in the total quantity.

3.2 Initial Value, Boundary Condition and Numerical Computation Method

The basic input parameters required for numerical computation of port flow characteristics include the following: cylinder bore diameter, stroke, maximum valve lift, and the inner diameter of the valve seat. The pressure boundary condition of the intake port was set at 100 kPa (total pressure), and the pressure data at the outlet of the intake port was taken as static pressure. The pressure differential between the inlet and the outlet of the port remained as a constant value, e.g., 6.5 kPa at low valve lift and 2.5 kPa at high valve lift. Port inlet air temperature was set at 293.15 K, turbulence length scale was set as 0.001 m, and boundary turbulent kinetic energy was $1m^2/s^2$. The initial conditions were set as follows: using port outlet pressure, no-slip on wall surfaces, adiabatic, and fixed wall surface temperature.

The steady-state method was used in numerical simulations. The Minmod Relaxed Difference scheme was used to solve the momentum conservation equation. A central difference scheme was adopted for the continuity equation. The same Minmod Relaxed Difference scheme, which has a second-order accuracy and superior convergence speed and stability, was used for the turbulence equation. The fluid in the model was compressible gas. Standard wall functions were used for surface treatment and wall heat transfer. The $k-\varepsilon$ double function model was used for the turbulence model. Standard residuals were used for convergence criteria. The maximum number of iterations in numerical computation was set at 3000. When the pressure, momentum, and turbulent kinetic energy residual reached less than 1e-4, the computation was considered to achieve steady convergence (He Changming, 2009).

4. SIMULATION AND EXPERIMENTAL RESULTS OF INTAKE PORT FLOW CHARACTERISTICS

Several simulation models were established to simulate different intake port combinations. The simulation results were compared to steady-state flow bench testing results, and correlations were obtained for port flow coefficients and swirl ratios at various valve lifts.

4.1 Scheme 1 (Combination of Left Helical Port and Right Tangential Port)

As shown in Fig. 6, the port flow coefficient of the combined ports increases with valve lift. The maximum deviation between testing and simulation, approximately 8%, occurs at the valve lift 3 mm. When the valve lift becomes greater, the deviation becomes very small, being less than 1%, i.e., the experimental curve and the simulation curve almost overlap each other.

As shown in Fig. 7, when the valve lift is less than 5 mm, the rate of increase of swirl ratio vs. valve lift is small, and the swirl ratio is only 0.63 when the valve lift is 5 mm. However, when the valve lift is greater than 5 mm, the swirl ratio substantially increases. When the valve lift reaches the fully open position, the swirl ratio becomes 1.16, and the flow coefficient becomes 0.65. The main reason is that at

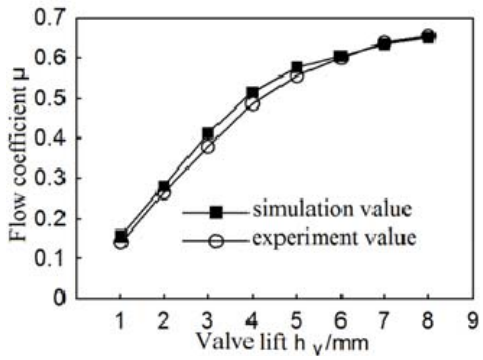

Fig. 6. The relationship between port flow coefficient and valve lift in Scheme 1.

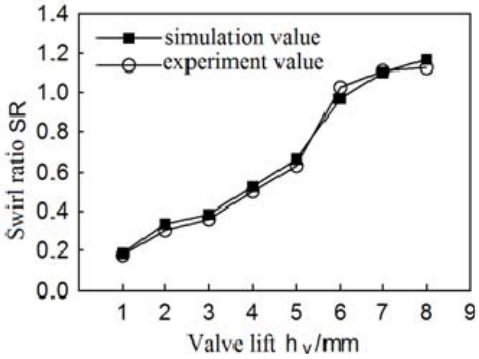

Fig. 7. The relationship between swirl ratio and valve lift in Scheme 1.

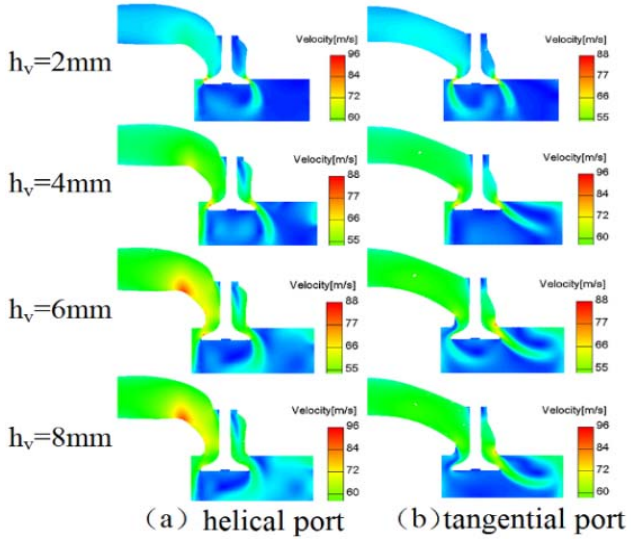

Fig. 8. Air flow velocity distribution of intake ports in Scheme 1.

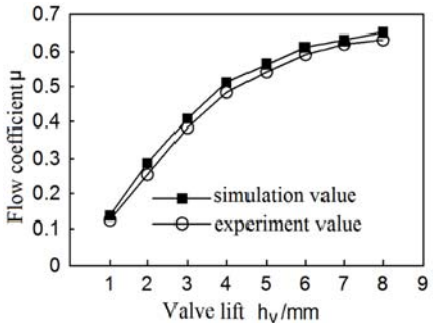

Fig. 9. The relationship between port flow coefficient and valve lift in Scheme 2.

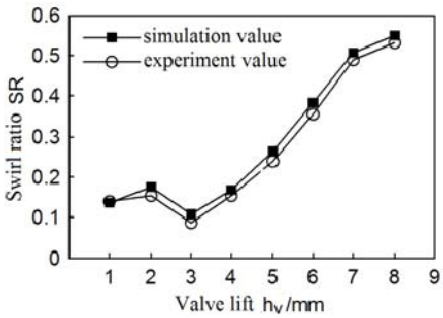

Fig. 10. The relationship between swirl ratio and valve lift in Scheme 2.

low valve lifts the effect of the helical port on swirl motion is strong, while at high valve lifts the helical effect becomes less prominent and the swirl motion is mainly affected by the flow of the tangential port. The air flow velocity distribution of the intake ports is shown in Fig. 8.

4.2 Scheme 2 (Combination of Left Tangential Port and Right Helical Port)

As shown in Fig. 9, the combined port flow coefficient increases with valve lift. The maximum discrepancy between testing and simulation is 8.5%, occurring at 2 mm valve lift.

As shown in Fig. 10, the swirl ratio has a sudden decrease at 3 mm valve lift due to stronger throttling effects and increased turbulence intensity near the throat of the port at this low valve lift. When the valve lift reaches the fully open position, the swirl ratio reaches the maximum value of 0.67, and the flow coefficient reaches 0.66. As the valve

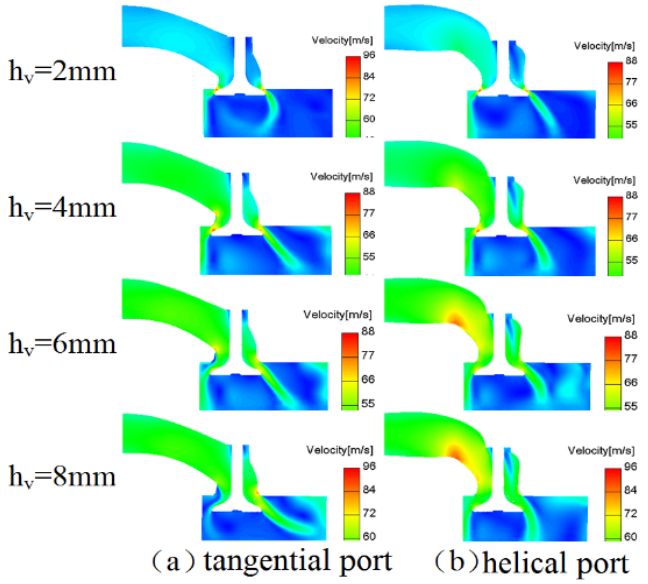

Fig. 11. Air flow velocity distribution of intake ports in Scheme 2.

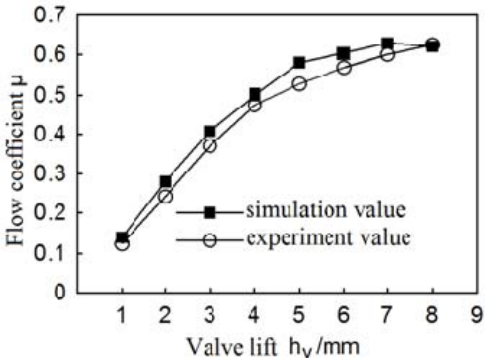

Fig. 12. The relationship between port flow coefficient and valve lift in Scheme 3.

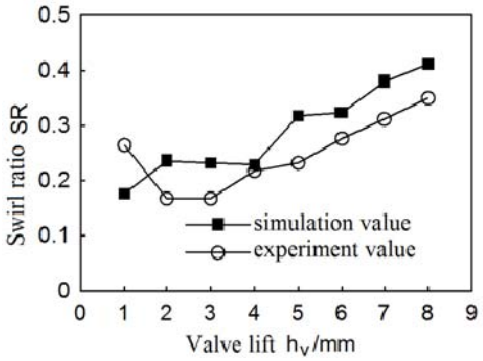

Fig. 13. The relationship between swirl ratio and valve lift in Scheme 3.

lift increases, the swirl ratio increases. However, the magnitude of increase is smaller than that of Scheme 1 due to the relatively weak capacity of the tangential port in generating swirls. The air flow velocity distribution of the intake ports is shown in Fig. 11.

4.3 Scheme 3 (Combination of Left Helical Port and Right Helical Port)

As shown in Fig. 12, when the valve lift is less than 5mm, the flow coefficient increases rapidly with valve lift. However, the flow coefficient increases at a much slower rate when the valve lift is greater than 5mm. The reasons for these phenomena are as follows. When the valve lift is less than 5 mm, the cross-section areas of the intake flow passages are relatively small and dominated by the effect of valve lift. Although the flow resistance of the double helical ports is large, its contribution to flow efficient is small. When the valve lift is greater than 5 mm, the cross-section areas of the intake flow passages are relatively large and dominated by the effect of helical port flow resistance. The maximum discrepancy between testing and simulation is 6.9%, occurring at 5 mm valve lift.

As shown in Fig. 13, the in-cylinder swirl strength caused by the double helical ports increases when the valve lift becomes greater, with the maximum swirl ratio being 0.41 and the maximum flow coefficient being 0.62, occurring at the fully open valve lift (8 mm). When the valve lift is around 2 mm and 3 mm, the swirl ratio is less, mainly due to the stronger interference effects between the two helical ports when the flow rate becomes lower atlow valve lifts. The air flow velocity distribution of the intake ports is shown in Fig. 14.

4.4 Scheme 4 (Combination of Left Tangential Port and Right Tangential Port)

As shown in Fig. 15, the combined port flow coefficient increases very fast, and the maximum flow coefficient is approximately 0.65. The main reason is that the flow resistance of tangential ports is very small, and the low resistance can enhance air flow rate. The maximum discrepancy between testing and simulation is 8.3%, occurring at 5 mm valve lift.

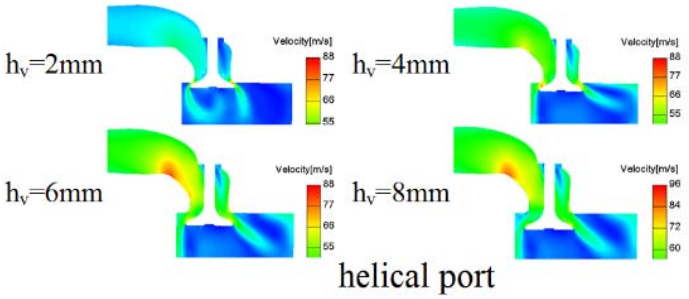

Fig. 14. Air flow velocity distribution of intake ports in Scheme 3.

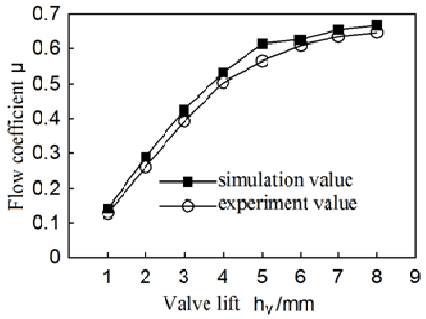

Fig. 15. The relationship between port flow coefficient and valve lift in Scheme 4.

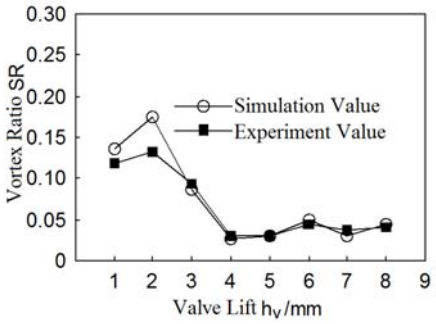

Fig. 16. The relationship between swirl ratio and valve lift in Scheme 4.

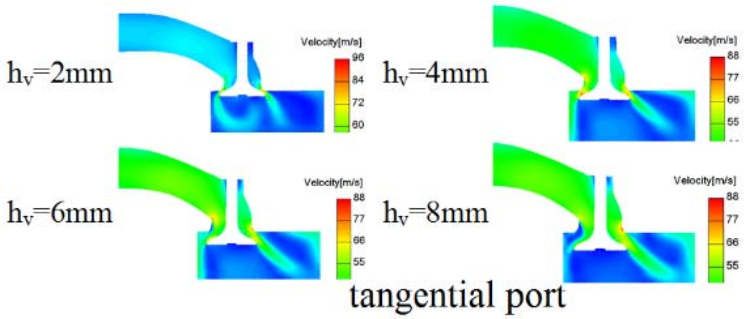

Fig. 17. Air flow velocity distribution of intake ports in Scheme 4.

As shown in Fig. 16, the swirl ratio is approximately 0.15 at low valve lifts, and it is lower compared to other port combination schemes. The swirl ratio is close to zero at high valve lifts because of weak swirl generation capacity of tangential ports. The air flow velocity distribution of the intake ports is shown in Fig. 17.

5. CONCLUSIONS

This work investigated the flow characteristics through the combined intake ports by 3D fluid simulation model and steady-state experiment. Each combined intake port has its own flow rule, but there are some common rules on the four combined intake ports.

(1) For the all four schemes of combination of intake ports, the port flow coefficient varies between 0.65 and 0.67 when the valve lift is the maximum. Due to the interference of intake flows of two ports, the swirl ratio varies greatly. The swirl ratio of the combined helical and tangential ports is the greatest among all different schemes.

(2) For the all four schemes of combination of intake ports, their port flow coefficients all increase with valve lift increasing. The swirl ratio of Scheme 1 increases with valve lift increasing, while the swirl ratio of Scheme 4 decreases with the valve lift increasing, and the swirl ratio is an almost zero when the valve lift is the maximum.

(3) The trend of numerical simulation of the port flow coefficients of the four schemes agrees well with experimental results, especially at the maximum valve lift. The simulation results of

swirl ratios of the four schemes exhibits slightly larger deviations compared with experimental results, but the simulation trend of the relationship between swirl ratio and valve lift is consistent with testing trend. Therefore, in order to master the flow characteristics laws of the intake ports, the 3D fluid simulation modeling and steady-state experiment are coupled to design and investigate intake ports.

ACKNOWLEDGEMENTS

This research was partially supported by the Chinese National Natural Science Foundation (No. 51105184) and the Basic Research Key Capital Projects of Yunnan Province (No. 2014FA026).

REFERENCES

Andreatta, É., F. Barbieri, L. Squaiella and R. Sassake (2008). *Intake Ports Development: Euro Ⅳ Diesel Engine Cylinder Head*. SAE Paper 36-0331.

Cantore, G., S, Fontanesi and V. Gagliardi (2005). *Effects of relative port orientation on the in-cylinder flow patterns in a small unit displacement HSDI Diesel Engine*. SAE Paper 32-0093.

Changming, H., B. Yuhua, L. Jilin and S. Lizhong (2009). A New Design Method for diesel Helical Intake Port Parameter.*Transaction of CSICE 27*(3) 265-269.

Choi, M., J. Song and S. Park (2016). Modeling of the fuel injection and combustion process in a CNG direct injection engine. *Fuel 179*, 168-178.

Cui, L., T. Wang, Z. Lu, M. Jia and Y. Sun (2015). Full-Parameter Approach for the Intake Port Design of a Four-Valve Direct-Injection Gasoline Engine. *Journal of Engineering for Gas Turbines and Power137*(9), 091502-091502-11.

Kawaguchi, A., T. Aiba, N. Takada and K. Ona (2009). A Robustness-Focused Shape Optimization Method for Intake Ports. *SAE Technical Paper* 2009-01-1777.

Kawashima, J., H. Ogawa and Y. Tsuru (1998). *Research on a Variable Swirl Intake Port for 4-Valve High-Speed DI Diesel Engines*. SAE Paper 982680.

Lu, Z., T. Wang, S. Liu, Z. Lin and Y. Han (2014). Experimental and Modeling Study of the Effect of Manufacturing Deviations on the Flow Characteristics of Tangential Intake Port in a Diesel Engine. *Journal of Engineering for Gas Turbines and Power 136*(11), 112101-112101-9.

Rathnaraj, J. D., B. J. Bose and P. M. Kumar (2006). *Simulation and experimental investigation of variable swirl intake port in DI Diesel Engine using CFD*. European Fluids Engineering Summer Meeting.

Sun, P., X. Kaiyan, X. Xuefeng and Z. Yanjing (2007). Numerical simulation and experiment on study flow test bench of diesel intake port. *Transactions of the Chinese society of agriculture engineering 23*(1), 99-104.

Torre, D., A. G. Montenegro and A. Onorati (2017). Coupled 1D-quasi3D fluid dynamic models for the simulation of IC engine intake and exhaust systems. In 17. *Internationales Stuttgarter Symposium* (1461-1476). Springer Vieweg, Wiesbaden.

Yufeng, L. and W. Zhong(2004). Experimental Study of Formation of Intake Swirl in the Cylinder of A 4-Valve Diesel Engine. *ACTA Armamentarii 25*(1), 113-115.

Yufeng, L., G. Xiaohui, W. Hai, L. Shuliang and X. Sidu (2001). Effects of Combination and orientation of Intake Ports on Swirl in Four-Valve DI Diesel Engines. *Transaction of CSICE 19*(3), 209-214.

Zhuang, H., and Hung, D. L. (2016). Characterization of the effect of intake air swirl motion on time-resolved in-cylinder flow field using quadruple proper orthogonal decomposition. *Energy Conversion and Management, 108*, 366-376.